One-step crystallization of InGaZnO thin film by spray pyrolysis for High performance Thin Film Transistor applications

Arqum Ali[1], and Jeong-Hwan Lee [1,2]

jeong-hwan.lee@inha.ac.kr
[1]Program in Semiconductor Convergence, Inha University, Republic of Korea
[2]Department of Materials Science and Engineering, Inha University, Republic of Korea
Keywords: Crystalline InGaZnO, High-Mobility, Thin-film Transistor.

ABSTRACT

We demonstrated as-grown crystalline InGaZnO (c-IGZO) thin film by spray pyrolysis at a substrate temperature of 425 °C without any subsequent crystallization process. The fabricated c-IGZO TFT exhibited high field effect mobility of 44.93 cm²/V·s, and excellent stability under positive bias temperature stress. Therefore, c-IGZO TFTs by spray pyrolysis are promising for low-cost, high-resolution display applications.

1 Introduction

IGZO is a leading amorphous oxide semiconductor, widely used in commercial displays due to its excellent electrical performances [1,2]. However, to meet the demands of next-generation high-resolution and large-area display backplanes, reliable devices with higher mobility are essential. The crystalline oxide channel layer has emerged as a highly effective strategy for achieving high-performance oxide TFTs [3-5]. To crystallize oxide thin films grown at room temperature, high-temperature annealing or excimer laser heating is generally required [7,8]. Although these techniques improve the mobility of IGZO TFTs, they require additional steps like prolonged high-temperature annealing to produce high-quality crystalline films. This leads to reduced manufacturing throughput, restricts the use of flexible substrates, and raises production costs. A metal capping layer has recently enabled low-temperature crystallization of oxide semiconductors, improving TFT mobility [8,9]. However, it requires an extra step to remove the capping layer after crystallization.

Furthermore, IGZO TFTs are mainly deposited through vacuum techniques like sputtering or atomic layer deposition [10, 11]. However, sputtering has difficulty controlling the chemical composition of as-deposited thin films due to the fixed chemical composition of sputtering targets. While ALD is typically a slow process, leading to longer processing time and lower throughput. Compared to vacuum-based deposition methods, spray pyrolysis is a low-cost setup for the deposition of large area thin films [12, 13]. Its material versatility enables deposition of a wide range of compounds. Moreover, spray pyrolysis offers deposition of thin films over large substrate areas compared to vacuum deposition which limits deposition area due to fixed chamber size. Furthermore, unlike the vacuum process, spray coating can be used for the direct growth of crystalline oxide semiconductors without any additional crystallization process [14-16]. This can reduce the manufacturing cost and increases throughput.

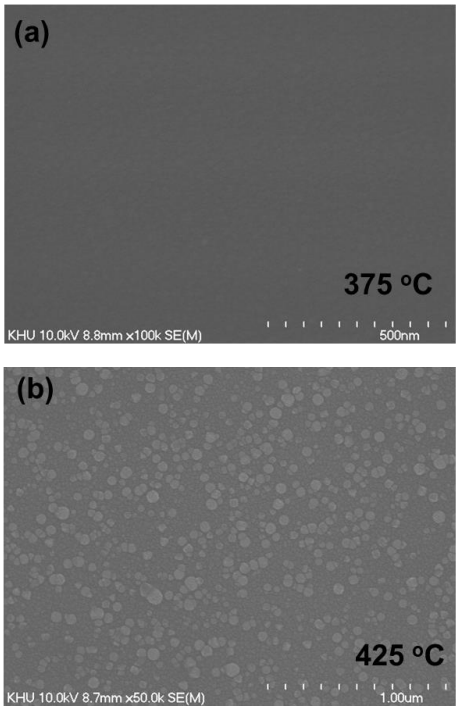

Fig. 1 SEM images of IGZO thin films deposited at substrate temperatures of (a) 375 and (b) 425 °C

In this work, we have successfully grown c-IGZO thin film directly on the preheated substrate by spray pyrolysis. The crystal structure of the IGZO thin film was confirmed by scanning electron microscope (SEM). The fabricated BCE c-IGZO TFT exhibits high field effect mobility of 44.93 cm²/V·s, and I_{ON}/I_{OFF} ratio of ~10^9 with no hysteresis. In addition, the threshold voltage shift is negligible when TFT stressed with the positive bias of 7 V at 60 ◦C. Therefore, spray coated c-IGZO TFT can replace the oxide TFTs by vacuum process due to its low-cost manufacturing over a large area.

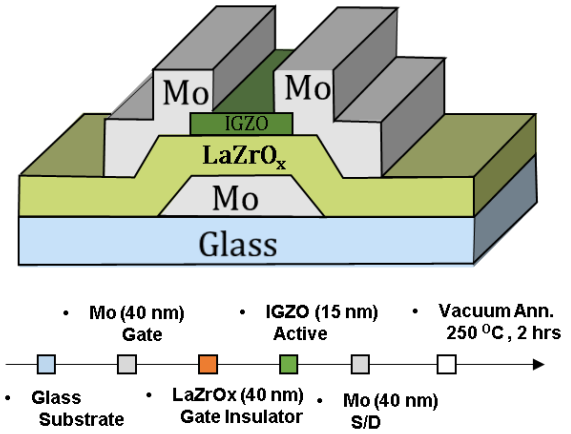

Fig. 2 Cross-sectional schematic of the fabricated bottom-gate top-contact IGZO TFT by spray pyrolysis.

2 Experiment

Indium chloride, gallium nitrate hydrate, and zinc acetate dehydrate were dissolved in 2-methoxyethanol at a 1:1:1 molar ratio to prepare 0.1 M IGZO solution. Ammonium acetate was added as a stabilizer to enhance solubility and film uniformity. All solutions were stirred for 2 h at room temperature under N2 ambient.

In this study, bottom-gate, top-contact TFT was fabricated as shown in Figure 2. First, 40 nm thick molybdenum (Mo) was sputtered and patterned as a gate electrode. Then 40 nm ZrO layer was deposited as a gate dielectric. Next, a 15 nm IGZO was deposited at 375 an d 425°C using spray pyrolysis and defined as an active island. Then, via holes were formed followed by the source and drain (S/D) electrodes defined with a 40 nm thick Mo layer

The TFTs were characterized by an Agilent 4156C semiconductor parameter analyzer at room temperature. To determine the gate and drain bias control, the transfer curve was measured at drain voltages (0.1-1.1 V) by sweeping the gate voltage from −5 to +7 V. The field effect mobility was determined from the transconductance parameter at V_{DS}=0.1V. The threshold voltage V_{TH} was considered to be the V_{GS} satisfying I_{DS}=W/L X 10pA. The SS was obtained from the linear region of the log (I_{DS}) versus VGS fitting using $(\partial \log I_D / \partial V_{GS})^{-1}$.

3 Results and Discussion

Figure 1 shows the SEM images of IGZO thin films deposited at substrate temperatures of 375 °C and 425 °C. As shown in Fig. 1(a), The IGZO thin film deposited at 375 °C demonstrates smooth and featureless surface morphology, indicating the amorphous nature of the IGZO thin film. In contrast, the film deposited at 425 °C (Fig. 1b) exhibits the formation of distinct and uniformly distributed grain-like features, confirming the in-situ crystallization of the IGZO thin film during deposition. The IGZO thin film deposited at 375 °C demonstrates amorphous structure due to insufficient thermal energy to drive crystallization. However, the deposition temperature of 425 °C provides enough thermal energy to promote nucleation and grain growth. Higher substrate temperatures increase particle mobility, promoting diffusion and migration, which in turn promote agglomeration resulting in well-defined crystalline structure [17].

Figure 3 shows the transfer characteristics of representative TFTs at a drain voltage (V_{DS}) of 0.1 and 1.1 V. IGZO TFT deposited at 375 ◦C (Fig 3a) exhibits the field effect mobility (μ_{FE}) of 29.09 cm²/V·s. The performance of TFT is significantly improved when the deposition temperature increases to 425 °C (Fig 3b), and IGZO TFT exhibits the μ_{FE} of 44.93 cm²/V·s. This enhancement is primarily due to the crystallization of IGZO [7,9,15]. The disorder induced trap states and scattering centers can be suppressed via lattice ordering, leading to enhanced carrier mobility [18,19]. The device parameters μ_{FE}, SS, and V_{TH} are summarized in Table I.

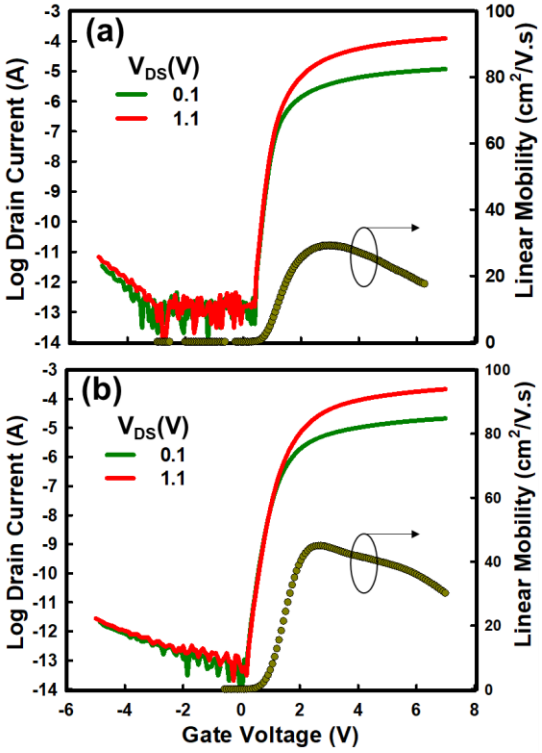

Fig. 3 Transfer characteristics of spray coated IGZO TFTs fabricated at (a) 375 °C (a-IGZO) and (b) 425 °C (c-IGZO).

Table I.

Table I: Summary of the electrical parameters of fabricated TFTs

Parameters	a-IGZO	c-IGZO
V_{TH} (V)	0.52	0.33
μ_{FE} (cm^2/V·s)	29.09	44.93
SS (mV/dec.)	106	139
PBTS (ΔV_{TH})	0.5	0.07

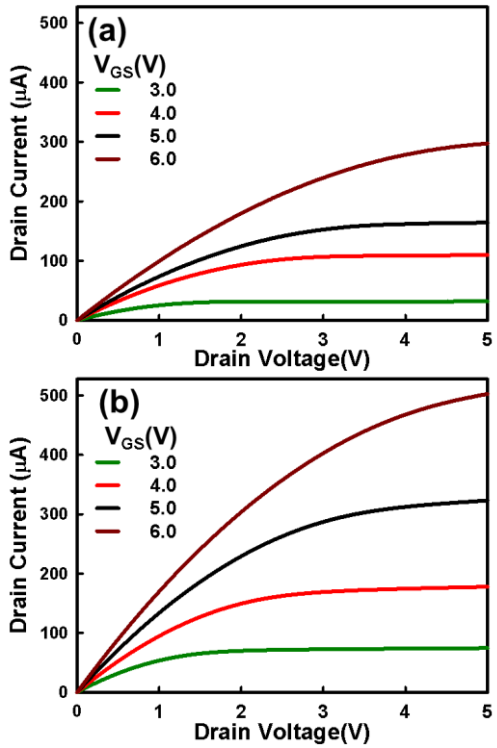

Fig. 4 Output characteristics of (a) a-IGZO and (b) c-IGZO TFTs.

The output characteristics of IGZO TFTs fabricated are shown in **Figure 4**, measured at various gate voltages (V_{GS} = 3.0–6.0 V). The device fabricated at 425 °C (Fig 1b) shows significantly higher drain current levels across all V_{GS} values than the device fabricated at 375 °C (Fig 1a), indicating enhanced carrier transport. This improvement is consistent with the observed crystallization at 425 °C, which promotes improved carrier mobility due to better atomic ordering and reduced trap density [20].

4 Conclusions

In conclusion, we successfully demonstrated the in-situ transformation of an a-IGZO into c-IGZO at the substrate temperature of 425 ºC by spray pyrolysis. The experimental results confirmed that the structural evolution of IGZO is strongly dependent on substrate temperature. The resulting c-IGZO TFT exhibited high field-effect mobility of 44.93 cm^2 /Vs with reliable bias stability. These findings highlight the strong potential of c-IGZO TFTs fabricated by spray pyrolysis for use in low-cost display applications.

Acknowledgment

This research was supported by Basic Science Research Program through the National Research Foundation of Korea(NRF) funded by the Ministry of Education(RS-2022-NR070869), and was also supported by the Digital Research Innovation Institution Program Through the National Research Foundation of Korea(NRF) funded by Ministry of Science and ICT (RS-2023-00283597).

References

1. Y. Xue, L. Wang, Y. Zhang, G. Liang, J. Chu, B. Han, W. Cao, C. Liao, and S. Zhang, IEEE Electron Device Lett., **2021**, 42, 188–191.
2. Y.Chen, D. Geng, J. Jang, IEEE Journal of the Electron Devices Society, **2018**, 6, 214-218.
3. T. Lim, S. Priyadarshi, S. Lee, J. Sun, J. Kim, B. Kim, S. Woo, S. Lee, J. Bae, Y. Kim, J. Koh, T. Kim, B. Kuh, J. Jang, IEEE Transactions on Electron Devices, **2025**, 75, 5.
4. M. Jeong, J. Bae, J. Kim, S. Priyadarshi, H. Lee, S. Woo, S. Moon, J. Jang, Adv. Mater. Technol. **2025**, e00561.
5. A. Ali, M. M. Islam, J. Jang, Adv. Mater. Technol. **2024**, 9, 2301778.
6. M. Nakata, K. Takechi, S. Yamaguchi, E. Tokumitsu, H. Yamaguchi, S. Kaneko, Jpn. J. Appl. Phys., **2009**, 48, 11.
7. H. J. Jeong, Y. S. Kim, S. G. Jeong, J. S. Park, ACS Appl. Electron. Mater. 2022, 4, 1343−1350
8. M. Nakata, K. Takechi, S. Yamaguchi, E. Tokumitsu, Y. Shin, S. T. Kim, K. Kim, M. Y. Kim, S. Oh, J. K. Jeong, Sci. Rep.,**2017**, 7, 1.
9. G. B. Kim, J. K. Jeong, ACS Appl. Mater. Interfaces **2025**, 17, 18677−18687.
10. J. Wu, H. Zheng, M. Guo, Y. Huang, X. Liang, Q. Wu, C. Liu. Journal of Alloys and Compounds, **2025**, 1022, 179753.
11. K. M. Lee, N. Kim, J. K. Lee , H. J. Lee, S. Y. Kim, T. G. Kim, Applied Surface Science, **2025**, 686, 162102.
12. A. Ali, M. M. Islam, M. M. Billah, S. Roy, B. Kim, M. H. Rabbi, J. Jang, Materials Letters, **2024**, 367, 136600.
13. H. Y. Liu, W. C. Hsu, J. H. Chen, P. H. Hsu, C. S. Lee, IEEE Transactions on Electron Devices, **2020**, 67, 3.
14. M. H. Rabbi, A. Ali, C. Park, J. Bae, J. Jang, Journal of Alloys and Compounds, **2024**, 1002, 175203.
15. J. Bae, A. Ali, M. M. Islam, M. Jeong, C. Park, J. Jang, ACS Appl. Mater. Interfaces **2023**, 15, 39494−39504.
16. A. Ali, M. M. Islam, J. Bae, J. Jang, IEEE Electron Device Letters, **2023**, 44, 10.
17. A. S. Bhoir, S. D. Gunjal, A. S. Pathan, A. S. Landge, Y. V. Hase, B. M. Palve, D. L. Gapale, S. A. Arote, Next Materials, **2024**, 5, 100272.
18. H.-Y. Liu, H.-C. Hung, and W.-T. Chen, IEEE Trans. Electron Devices, **2020**, 67, 4245–4249.
19. B. K. Kim, N. On, C. H. Choi, M. J. Kim, S. Kang, J. H. Lim, J. K. Jeong, IEEE Electron Device Lett., **2021**, 42, 347–350.
20. Z. Chen, Z. Fu, T. Jin, L. Jing, J. Ren, M. Lei, J. Sun, H. Chen, L. Liang, H. Cao, Appl. Phys. Lett. **2025**,126, 033504.